

Assessment of Neutron Contamination Originating from the Presence of Wedge and Block in Photon Beam Radiotherapy

Bahreyni Toossi M. T.¹, Khajetash B.^{1*}, Ghorbani M.¹

ABSTRACT

Background: One of the main causes of induction of secondary cancer in radiation therapy is neutron contamination received by patients during treatment.

Objective: In the present study the impact of wedge and block on neutron contamination production is investigated. The evaluations are conducted for a 15 MV Siemens Primus linear accelerator.

Methods: Simulations were performed using MCNPX Monte Carlo code. 30°, 45° and 60° wedges and a cerrobend block with dimensions of 1.5 × 1.5 × 7 cm³ were simulated. The investigation were performed in the 10 × 10 cm² field size at source to surface distance of 100 cm for depth of 0.5, 2, 3 and 4 cm in a water phantom. Neutron dose was calculated using F4 tally with flux to dose conversion factors and F6 tally.

Results: Results showed that the presence of wedge increases the neutron contamination when the wedge factor was considered. In addition, 45° wedge produced the most amount of neutron contamination. If the block is in the center of the field, the cerrobend block caused less neutron contamination than the open field due to absorption of neutrons and photon attenuation. The results showed that neutron contamination is less in steeper depths. The results for two tallies showed practically equivalent results.

Conclusion: Wedge causes neutron contamination hence should be considered in therapeutic protocols in which wedge is used. In terms of clinical aspects, the results of this study show that superficial tissues such as skin will tolerate more neutron contamination than the deep tissues.

Keywords

Neutron contamination, wedge, cerrobend block, Siemens Primus linac, Monte Carlo simulation

Introduction

Cancer is a leading cause of death worldwide, according to the World Health Organization (WHO) report, about 8.2 million deaths dedicated in 2012 in the world [1]. There are several modalities for treatment of cancer. Some of them are surgery, chemotherapy, radiation therapy, hormonal therapy and immunotherapy [2]. Based on radiotherapy protocols there are cases in which beam modification devices are used during radiation therapy fractions. The most important beam modification devices are block, wedge filter, flattening filter, multileaf collimator and asymmetric jaws.

¹Medical Physics Department, Faculty of Medicine, Mashhad University of Medical Sciences, Mashhad, Iran

*Corresponding author: B. Khajetash, Medical Physics Department, Faculty of Medicine, Mashhad University of Medical Sciences, Paradise Daneshgah, Vakil Abad Blvd., Mashhad, Iran
E-mail: Benyamin.khajetash@gmail.com

Received: 20 December 2015
Accepted: 6 March 2016

Recently, there has been worry about second cancer induction related to radiation therapy. One of the most important factors in developing a second cancer is neutron contamination production in megavoltage beam radiation therapy [3]. Using megavoltage accelerator has two main advantages: lower skin dose and higher dose rate in treatment of deep tumors. However, a disadvantage of the megavoltage beams is undesired fast neutrons production. Neutrons have significant biological damage, due to their high weighting factor (W_R) according to International Commission on Radiological Protection (ICRP) report No. 60 [4]. Neutrons are produced by photonuclear interactions when the photon energy is higher than the threshold energy of the (x, n) reaction [5]. This threshold energy depends on the atomic number of the material. There are high atomic number elements in components of the accelerator's head such as collimator, jaws and flattening filter, etc. Wedge filters and blocks are usually made of heavy metals such as lead, tungsten or steel (which are good beam absorbers). In conventional radiotherapy, presence of wedge and block in the path of the primary beam can generate neutron contamination. In addition, the head components of various models of accelerators are different and this makes differences in neutron contamination by different accelerators.

Hashemi, et al [6] studied the impact of wedge in increasing the neutron contamination in 18 MV photon beam of Varian 2100 C/D linac. In that study, polycarbonate film was used to measure the neutron dose. The results indicated that by taking into account the wedge factor, 54 % neutron dose enhancement was observed on the central axis. There was neutron dose reduction with increasing distance from central axis up to the distance of 50 cm.

Mesbahi, et al [7] examined the effect of wedge filter and the field size on neutron dose

equivalent. In their study 18 MV photon beam of Elekta SL75/25 accelerator simulation modeling was performed by MCNPX Monte Carlo code. A 60° wedge filter made of lead alloy was modeled. The results showed that, in the presence of the wedge, neutron dose equivalent was increased 6.5 times, on average. For open field, neutron dose equivalent decreased with increasing the field size, while in the wedged field, the neutron dose equivalent increased with increasing the field size. Furthermore, for both open and wedged field, neutron dose equivalent reduced with increasing the distance from the central axis of the beam.

Biltekin, et al [8] evaluated the wedge filter effect on neutron contamination in 18 MV photon beam of Elekta Synergy Platform and 18 MV photon beam of Varian Clinac DHX High Performance linear accelerators. Bubble detector personal neutron dosimeter (BD-PND) was used to measure the neutron contamination. Measurements were performed in open and wedged fields with 30 degrees wedge. The results showed 62.4 % and 17.8 % increase in neutron dose equivalent compared with the open field for Elekta and Varian linear accelerators, respectively.

Hashemi, et al [9] investigated the effect of block modifier for Elekta SL 75/25 (18 MeV photon beam) and Saturn 43 (25 MeV photon beam) linacs. In their study Polycarbonate film was applied in order to measure the neutron contamination. Results showed increased neutron dose equivalent on central axis of about 28 % and 21 % for Elekta (18 MeV) and Saturn (25 MeV) (in presence of block), respectively. In addition, with moving away from the isocenter to 50 cm distance, the neutron dose equivalent decreases rapidly for both open and blocked fields.

In addition to aforementioned studies, other studies have been performed in the field of neutron contamination evaluation [10-15]. In

most of these studies neutron dose was measured in air and the effect of phantom material were not considered. In terms of clinical aspects, knowing the neutron dose in-vivo (or in phantom as the representative of human body) is essential. To the best of our knowledge, the effect of wedge and block in photon-neutron contamination production for Siemens Primus linac has not been studied. The aim of this study is to assess the wedge and cerrobend block effect on neutron contamination production inside the phantom with 15 MV photon beams of a Siemens Primus linear accelerator. Three wedges (30°, 45° and 60°) and cerrobend block modifier are investigated in order to evaluate neutron dose in different in-phantom depths.

Materials and Methods

Validation of linac simulation

Validation of Siemens Primus linear accelerator simulation was conducted by the colleagues of the present project based on a previous study [11]. Herein a brief review of the previous work is presented. The 15 MV photon beam of a Siemens Primus medical linear accelerator (Siemens AG, Erlangen, Germany) was simulated based on the manufacturer's geometric information. In that study, MCNPX code (version 2.6.0.) was used. Then, the percentage depth dose data were determined for three field sizes (6 × 6 cm², 10 × 10 cm² and 18 × 18 cm²). Furthermore, dose profiles were investigated for these three fields at depths of 5, 10 and 20 cm in a water phantom.

To perform dose calculations a water phantom was used. The dimensions of the water phantom were 30 × 30 × 30 cm³ and the phantom was defined at source to surface distance (SSD) of 100 cm. Measurements were performed using a Wellhöfer-Scanditronix dosimetry system (Wellhöfer, Uppsala, Sweden)

and a water phantom (RFA-300; IBA Dosimetry GmbH, Schuarzenbruck, Germany) at the Reza Radiation Oncology Centre (Mashhad, Iran). In-phantom depth measurements were performed using a diode detector. The comparison of Monte Carlo calculation and measurement data was carried out by gamma function. Gamma calculations were performed using dose difference and distance to agreement criteria of 3 % and 3 mm, respectively. Gamma function criteria indicated good agreement between the results by Monte Carlo calculations and in-phantom measurements.

Geometry of wedges and block

Three wedges (30°, 45° and 60°) were simulated. The 30° wedge has 5 layers and 45° and 60° wedges have 4 layers. According to manufacturer information the material of these wedges is EZcut20 steel. The heights of the heels of the wedges are 2.97, 5.61 and 5.99 cm for 30°, 45° and 60° wedges, respectively. These wedges are attached to a tray. The tray dimensions were approximately 20 × 20 × 0.5 cm³ and it is made of aluminum. A cerrobend block was also made for investigating the block effect. Its composition was analyzed by atomic absorption method (by XplorAA Atomic Absorption Spectrometer, manufactured by GBC Australia) in Khorasan Science and Technology Park (KSTP). The percentage composition of the block is listed in Table 1. Cerrobend density was obtained as 9.41 g/cm³. The block dimensions are 1.5 × 1.5 × 7 cm³ that was stuck to a perspex tray. This perspex tray has dimensions of about 20 × 20 × 1 cm³. Density of 1.19 g/cm³ was used for perspex in the simulations.

Effect of wedge and block on neutron contamination

In this study, the validated program of 15 MV Siemens Primus linac installed at Reza Radiation Oncology Centre (Mashhad, Iran) that was mentioned in the previous section

Table 1: Compositions (weight fraction) of cerrobend obtained by atomic absorption spectrophotometry method

Element	Percentage (%)
Tin (Sn)	21.31
Lead (Pb)	26.34
Bismuth (Bi)	52.35

was used. Calculations were performed at a source to surface distance of 100 cm with 10×10 cm² field size. Neutron dose in a water phantom with dimensions of $30 \times 30 \times 30$ cm³ was calculated at four depths of 0.5, 2, 3 and 4 cm. MCNPX Monte Carlo code (version 2.6.0) was utilized [16]. The wedge and block trays were placed at distances of 41.5 cm and 51.5 cm from the target, respectively. The neutron dose was scored in cylindrical cells which had 1 cm height and 1.5 cm radius.

If electron spectrum was used as the source and thereafter the neutron dose was scored, the uncertainties and the time needed for running of the programs could be high. In addition, it is not feasible to run more than 2 billion particles in a single program in the MCNPX code. Therefore, a two-step process was followed which will be described in the following.

In the first stage, a sphere of air with 1 cm diameter was defined above the flattening filter, while its center was located at distance of 3.7 cm below the electron source. All accelerator components including target, primary collimator, absorber, flattening filter, photon dose chamber, Y and X jaws and $30 \times 30 \times 30$ cm³ water phantom was defined in this stage. The validated electron spectrum was used in this program, and then F4 tally was scored in order to achieve the photon flux in various energy bins. In order to reduce the related uncertainties the 0.5 energy bins were considered. In order to reduce the run time, energy cut off of 10 keV was defined for both electron and photon. In this program, the number of tracked particles was 2.75×10^8 and the maximum un-

certainty at this stage was 70 %. This uncertainty is related to the last photons energy bin, and it is high because the number of photons was very low in this energy bin. The number of photons in this last energy bin was about 10^3 times less than the number at previous energy bins, thus the last bin uncertainty has no effect on the accuracy calculation. In the other energy bins the uncertainty was less than 1 %.

In the second stage, a photon source was defined at above the target in the form of a cone with 20 degrees vertex angle. Furthermore, in contrast to the previous program the target and absorber were ignored and replaced with air. The obtained photon flux in the first program was applied as an input photon source spectrum in this stage. Calculations for five cases (open field, 30°, 45° and 60° wedges and blocked field) were performed in the same condition. For all the cases, source to surface distance of 100 cm and phantom dimensions of $30 \times 30 \times 30$ cm³ was considered. Since photonuclear reaction occurs in energies upper than 8 MeV photon energy for elements of high atomic number, energy cut off of 7 MeV was considered for photons and electrons. Energy cut off of 10 keV was used for neutrons due to the fact that most of the produced neutrons are fast neutrons. Moreover, each program was run for 2×10^8 particles. In order to reduce the calculation uncertainties to less than 10 %, each case was run in 13 input programs. Due to high uncertainty in the cerrobend block program, this program was run 30 times. All programs were in the same condition, but in each program random, seed number was changed to increase the precision and to obtain various outputs.

According to the following equation the total uncertainty was calculated:

$$\text{Total uncertainty} = \sqrt{\left(\frac{n_1}{N}\right)^2 \sigma_1^2 + \left(\frac{n_2}{N}\right)^2 \sigma_2^2 + \dots + \left(\frac{n_m}{N}\right)^2 \sigma_m^2}$$

where n_1, n_2, \dots are the number of particles in each program and m is the program num-

ber. N is the total number of particles in all programs. σ_1 , σ_2 , etc. are uncertainties in the program number 1, number 2, etc.

In this study, results of two tallies were compared. F4 tally was used to obtain neutron flux (number of particles in a cell) and the flux was then converted to dose (rem) using DE and DF cards extracted from Table H-2 of MCNPX (version 2.6.0) manual. This table has two references for the conversion coefficients that American National Standards Institute (ANSI/ANS 6.1.1) reference values were used. F6 tally, that calculates energy per unit mass (kerma), was used to obtain neutron dose directly. The maximum Monte Carlo statistical total uncertainty in the tallies cells was 8 %. All of the wedge and block cases were compared to the open field and the relative neutron dose was achieved. Herein, the relative neutron dose is neutron dose at the specified depth in water phantom in presence of wedge or block to neutron dose at the same depth in open field. Neutron contamination was assessed in 4 depths in the water phantom (0.5, 2, 3 and 4 cm) and the results were compared. When F4 tally was used the relative neutron dose was obtained in terms of mSv per mSv and for the cases that F6 tally was used, the relative neutron dose was obtained in terms of cGy per cGy.

Results

The values of relative neutron dose for 30°, 45° and 60° wedges and cerrobend block are listed in Table 2. These values were obtained without considering wedge factors and block tray factor. To better evaluate the wedge and block effect on neutron contamination production, wedge and block tray factors were also applied. The wedge and block tray factors are shown in the Table 3. Values of relative neutron dose with considering the wedge/tray factors are presented in Table 4.

The calculated relative neutron dose ver-

Table 2: Relative neutron dose values (mSv/mSv) for 30°, 45° and 60° wedges and cerrobend block at 0.5, 2, 3 and 4 cm depths in 10 × 10 cm² field size without taking wedge/tray factor into account

Depth (cm)	30° Wedge	45° Wedge	60° Wedge	Block
0.5	0.70	0.57	0.57	0.50
2.0	0.65	0.55	0.54	0.48
3.0	0.67	0.54	0.55	0.45
4.0	0.62	0.49	0.50	0.49

Table 3: Wedge factors related to 30°, 45°, 60° wedges and block tray for 10 × 10 cm² field size of 15 MV photon beam of siemens primus linac

Wedge/Tray Factor	
30° Wedge	0.60
45° Wedge	0.40
60° Wedge	0.43
Block Tray	0.96

Table 4: Relative neutron dose values (mSv/mSv) for 30°, 45° and 60° wedges and cerrobend block at depths of 0.5, 2, 3 and 4 cm in 10 × 10 cm² field size with taking wedge/tray factor into account

Depth (cm)	30° Wedge	45° Wedge	60° Wedge	Block
0.5	1.16	1.42	1.33	0.51
2.0	1.09	1.37	1.25	0.49
3.0	1.12	1.35	1.29	0.47
4.0	1.04	1.22	1.17	0.51

sus depth for different wedges and cerrobend block are plotted in Figure 1 and Figure 2 by ignoring and taking into account the wedge/tray factor, respectively.

As it was mentioned in Materials and Methods section, two tallies (F4 and F6) were scored and their results are listed in Table 5.

In addition, the total statistical uncertainties in Monte Carlo calculations are listed in Table 6 in order to have a more detailed comparison for these tallies.

Discussion

In the present work, the relative neutron dose was calculated by MCNPX Monte Carlo code at various depths in water phantom for 30°, 45° and 60° wedges and a cerrobend block beam modifier. The results show neutron contamination enhancement in the presence

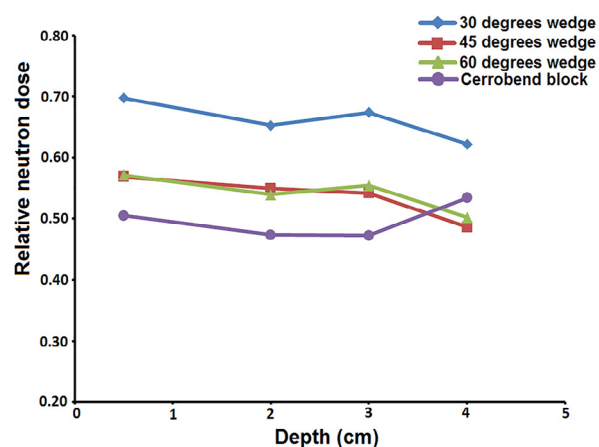


Figure 1: Relative neutron dose versus depth in water phantom without taking wedge/tray factor into account

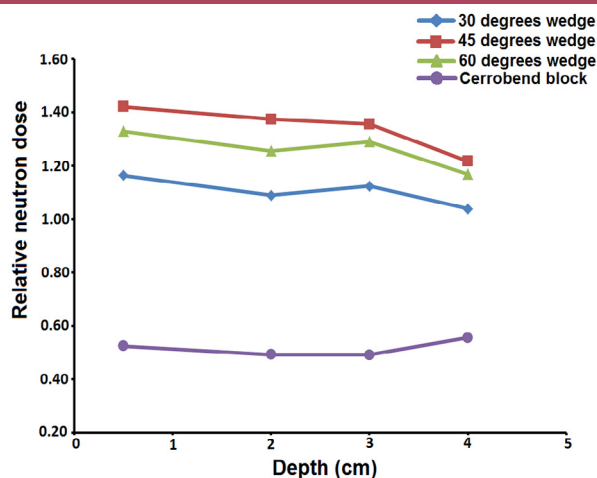


Figure 2: Relative neutron dose versus depth in water phantom without taking wedge/tray factor into account

of wedge when the wedge factor considered. Therefore, in the treatment protocols that the wedges are inevitably used as part of treatment, this additional neutron dose from external wedges located in the beam path should be taken into account. Neutrons can be a contribution to the integral dose and because of their high quality factor, even a small physical neutron dose can cause biological effects [17].

By comparing the data contained in Table 2 and Table 4, it can be seen that without con-

Table 5: Values of relative neutron dose by F4 and F6 tallies at different depths for 30°, 45° and 60° wedges and cerrobend block in water phantom with and without taking wedge/tray factor into account

Depth (cm)	Without taking wedge/tray factor into account								
	F4 Tally (mSv/mSv)				F6 Tally (cGy/cGy)				
	30° wedge	45° wedge	60° wedge	Block	30° wedge	45° wedge	60° wedge	Block	
0.5	0.70	0.57	0.57	0.50	0.70	0.56	0.57	0.51	
2.0	0.65	0.55	0.54	0.48	0.63	0.53	0.53	0.52	
3.0	0.67	0.54	0.55	0.45	0.65	0.53	0.55	0.49	
4.0	0.62	0.49	0.50	0.49	0.59	0.47	0.49	0.51	
Depth (cm)	With taking wedge/tray factor into account								
	0.5	1.16	1.42	1.33	0.51	1.16	1.41	1.31	0.53
	2.0	1.09	1.37	1.25	0.49	1.04	1.31	1.22	0.54
	3.0	1.12	1.35	1.29	0.47	1.08	1.31	1.29	0.51
	4.0	1.04	1.22	1.17	0.51	0.98	1.16	1.13	0.53

Table 6: Monte Carlo type A statistical uncertainty (%) for the F4 and F6 tallies in 0.5, 2.0, 3.0 and 4.0 cm depths in water phantom

Depth (cm)	Open field		30° wedge		45° wedge		60° wedge		Block	
	F4	F6	F4	F6	F4	F6	F4	F6	F4	F6
0.5	2.08	2.11	2.52	2.57	2.78	2.82	2.76	2.80	1.90	1.89
2.0	5.23	5.57	6.07	6.30	6.62	6.97	6.78	7.24	5.00	4.85
3.0	6.37	6.88	7.36	7.86	8.09	8.74	8.38	9.13	6.87	6.51
4.0	7.58	8.02	7.90	8.37	8.80	9.32	9.02	9.60	8.72	8.49

sidering wedge factors, relative neutron dose is not considerable. But in practice, if there is a wedge in the path of primary photon beam, to compensate the beam absorption that occurs in the presence of wedge, the number of monitor unit is increased. Therefore, in a constant monitor unit (in the current study as 100 MU) a compensating factor should be considered for a wedged field. As it is evident from Table 4, with considering the wedge factor in the calculations, there is neutron dose enhancement in presence of wedge. As it can be seen in Table 4, the relative neutron dose at depth of 0.5 cm for 45° wedge is equal to 1.42 (mSv/mSv), this means that 42 % neutron dose enhancement exist when a 45° wedge is used compared to the open field.

As it can be seen from the data in Table 2, for all cases the depth increase leads to reduction of neutron contamination. Both absorption and production of neutrons occur in the phantom. This effect is probably due to the fact that phantom contains hydrogen atoms and these hydrogen atoms are neutron absorbers. In addition, with increasing depth in the water phantom, the volume of the portion of phantom which located at the top of the dose calculation point increases, therefore, more neutrons are absorbed. By taking into account the wedge factors presented in Table 3, it can be seen in Table 4 that relative neutron dose reduces with depth increasing, similar to the previous trend. In terms of clinical application, the results of this study show that superficial tissues such as skin will tolerate more

neutron contamination.

As it can be seen in Figure 1, when the wedge factor was not considered, the most neutron contamination is produced by 30° wedge and the least contamination is associated with block. Additionally, the amounts of relative neutron dose are approximately equal for 60 and 45 degrees wedges. With considering wedge factors, as it can be seen in Figure 2, the effect of wedge on neutron contamination production is more prominent, compared to without application of the wedge factor. As it can be seen in Figure 2, the most neutron contamination is produced by 45° wedge that could be due to the fact that the wedge factor for this wedge is lower than the others. Since the wedge factors are lower than unity and the neutron dose is divided by wedge factor, a lower wedge factor corresponds to a higher neutron contamination for the 45 degrees wedge. According to this figure, after the 45 degrees wedge, 60 and 30 degrees wedges create the higher neutron contamination, respectively. Finally, the lowest neutron contamination is for the cerrobend block based on the diagram in Figure 1. Low neutron contamination from the block may be due to this fact that in the blocked field the total volume which is irradiated by photons is much less than in the wedged field.

As it was mentioned in the previous section, the results by F4 and F6 tallies are compared. As it can be seen from the data in Table 5, relative neutron dose values by F4 and F6 tallies at different depths for 30°, 45° and 60° wedges

and cerrobend block are relatively equal. The total Monte Carlo uncertainties of these tallies are listed in Table 6. As it can be seen from Table 6, while the numbers of particles scored in the program for these tallies are equal, the uncertainty values have less than 0.5 % difference and the maximum uncertainty is related to the depth of 4 cm. These points imply that the results by these tallies for neutron dose calculation are practically equal and both tallies will have the same uncertainties with similar scored number of particles (or similar running times for the input files).

In the study by Hashemi, et al [9], effect of lead block field modifier for Saturn 43 (25 MeV) and an Elekta SL 75/25 (18 MeV) linear accelerators was evaluated. In that study, increasing in the neutron dose equivalent on the central axis in presence of block of about 28 % and 21 % for Elekta (18 MV) and Saturn (25 MV) was reported, respectively, in contrast to our study. This difference maybe is due to the fact that in the present study, a small block was put in the middle of the field, while in that study blocks was placed around the field and smaller field was shaped. In addition, the composition of block, the model of accelerator and photon energy in that study are different from the current study. In the present study a cerrobend block was used, while in that study lead block was used. In that study, measurements were performed in the air and therefore the impact of phantom on neutron production was not considered contrary to the present study.

The results in Table 2 shows the difference with the study by Hashemi, et al [6]. They showed that the photoneutron dose equivalent increases in presence of wedge at central axis without considering wedge factor, for Varian 2100 C/D 18 MV linac. The reason of this difference may be because the measurements were performed in air in that study but calculations were performed in water phantom in

presence study. Additionally, the models of the linacs and wedge structures are different. Furthermore, in that study the external wedge was placed reversely compared to the current study. However, the results listed in Table 4 are in agreement with the results of that study. This data shows that neutron contamination increases in presence of wedge.

Biltekin, et al [8] findings indicate an increase in neutron dose equivalent in the presence of 30° wedge in 10 × 10 cm² field size for Varian and Elekta linacs. Their results are in good agreement with our results for Siemens Primus linac and 30° wedge in 10 × 10 cm² field size, presented in Table 4. In this table, it can be seen that the percentage increase in relative neutron dose for 30° wedge at depths of 0.5, 2, 3 and 4 cm are 16, 9, 12 and 4 percent, respectively.

The present study devoted to calculate the relative neutron dose only in 4 depths in water phantom at 10 × 10 cm² field size for 15 MV Siemens Primus linac. It is suggested that calculations be performed in more depths in a tissue equivalent phantom. Evaluation of the impact of phantom size and different field sizes on photoneutron contamination production is recommended. In addition, absolute dosimetry for better study of neutron contamination in phantom is suggested as a subject for future studies in this field.

Conclusion

The results showed increasing neutron dose in presence of wedge. It was also shown that with increasing depth, relative neutron dose reduced. Furthermore, the presence of cerrobend block in the center of the field causes less neutron contamination than the open field.

It is recommended that alternative treatment planning protocols be used to reduce neutron contamination and neutron contamination dose received by patients be considered during

treatment planning. Study on the structure and material that eliminate or minimize these undesirable photoneutrons can be suggested as future evaluations in this field. The results by F4 and F6 tallies for neutron dose calculation are practically equal and both tallies show the same uncertainties with similar scored number of particles (or similar running times for the input files).

Acknowledgment

This study is part of a M. Sc. thesis in the Medical Physics. The authors are grateful from Mashhad University of Medical Sciences (MUMS) for financial support of this work.

Conflict of Interest

There is not any relationship that might lead to a conflict of interest. Mashhad University of Medical Sciences (MUMS) has financially supported the work and this is stated in the acknowledgment section of the article.

References

1. In: World Health Organization. IARC-International Agency for Research on Cancer. [2014]. Available from: http://www.who.int/ionizing_radiation/research/iarc/en/.
2. Price P, Sikora K. *Treatment of Cancer, Sixth Edition*. London: CRC Press; 2014.
3. Exposito MR, Sanchez-Nieto B, Terron JA, Domingo C, Gomez F, Sanchez-Doblado F. Neutron contamination in radiotherapy: estimation of second cancers based on measurements in 1377 patients. *Radiother Oncol*. 2013;**107**:234-41. doi.org/10.1016/j.radonc.2013.03.011. PubMed PMID: 23601351.
4. Protection ICoR. ICRP Publication 60: 1990 Recommendations of the International Commission on Radiological Protection: Amsterdam: Elsevier Health Sciences; 1991.
5. In: National Council on Radiation Protection Measurements. NCRP Report 79, Neutron contamination from medical electron accelerators. [1984]. Available from: <http://ncrponline.org/publications/reports/ncrp-report-79/>.
6. Hashemi S, Raisali G, Taheri M, Majdabadi A, Ghafoori M. The effect of external wedge on the photoneutron dose equivalent at a high energy medical linac. *Nukleonika*. 2011;**56**:49-51.
7. Hashemi SM, Hashemi-Malayeri B, Raisali G, Shokrani P, Sharafi AA, Torkzadeh F. Measurement of photoneutron dose produced by wedge filters of a high energy linac using polycarbonate films. *J Radiat Res*. 2008;**49**:279-83. doi.org/10.1269/jrr.07066. PubMed PMID: 18460824.
8. Biltekin F, Ozyigit G, Yeginer M, Celik D, Gurkaynak M. EP-1376 investigating the effect of wedge filter on neutron contamination by using bubble detectors. *Radiotherapy and Oncology*. 2012;**103**:S522. doi.org/10.1016/S0167-8140(12)71709-7.
9. Hashemi SM, Hashemi-Malayeri B, Raisali G, Shokrani P, Sharafi AA, Jafarizadeh M. The effect of field modifier blocks on the fast photoneutron dose equivalent from two high-energy medical linear accelerators. *Radiat Prot Dosimetry*. 2008;**128**:359-62. doi.org/10.1093/rpd/ncm421. PubMed PMID: 17875628.
10. Mesbahi A. A Monte Carlo study on neutron and electron contamination of an unflattened 18-MV photon beam. *Appl Radiat Isot*. 2009;**67**:55-60. doi.org/10.1016/j.apradi-so.2008.07.013. PubMed PMID: 18760613.
11. Bahreyni Toossi MT, Behmadi M, Ghorbani M, Gholamhosseinian H. A Monte Carlo study on electron and neutron contamination caused by the presence of hip prosthesis in photon mode of a 15 MV Siemens PRIMUS linac. *J Appl Clin Med Phys*. 2013;**14**:52-67. PubMed PMID: 24036859.
12. Hussien M, Ma A, Spyrou N. Monte Carlo Simulations of the Effective Neutron Dose Received by a Male Anthropomorphic Voxel Phantom outside a Medical Linac Treatment Room. University of Surrey, Guildford, Surrey. 2006.
13. Zanini A, Durisi E, Fasolo F, Ongaro C, Visca L, Nastasi U, et al. Monte Carlo simulation of the photoneutron field in linac radiotherapy treatments with different collimation systems. *Phys Med Biol*. 2004;**49**:571-82. doi.org/10.1088/0031-9155/49/4/008. PubMed PMID: 15005166.
14. Hashemi SM, Hashemi-Malayeri B, Raisali G,

- Shokrani P, Sharafi AA, Torkzadeh F. Measurement of photoneutron dose produced by wedge filters of a high energy linac using polycarbonate films. *J Radiat Res.* 2008;**49**:279-83. doi.org/10.1269/jrr.07066. PubMed PMID: 18460824.
15. Zabihinpoor S, Hasheminia M. Calculation of Neutron Contamination from Medical Linear Accelerator in Treatment Room. *Adv Studies Theor Phys.* 2011;**5**:421-8.
16. Pelowitz D. MCNPX user's manual, version 2.6.0, LA-CP-07-1473. . New Mexico: Los Alamos National Laboratory; 2008.
17. Schneider U. Modeling the risk of secondary malignancies after radiotherapy. *Genes (Basel).* 2011;**2**:1033-49. doi.org/10.3390/genes2041033. PubMed PMID: 24710304. PubMed PMCID: 3927608.